High thermal resistance of γ-Al_2O_3 prepared by the selective leaching of calcined kaolin minerals

Yoshitoshi Saito, Takayuki Motohashi, Shigeo Hayashi, Atsuo Yasumori and Kiyoshi Okada*

Department of Inorganic Materials, Tokyo Institute of Technology, O-okayama, Meguro, Tokyo 152, Japan

The thermal resistance of mesoporous γ-Al_2O_3 prepared by selective leaching of calcined kaolin minerals has been investigated. γ-Al_2O_3 prepared from four types of kaolin minerals calcined at 950 °C for 24 h followed by leaching with KOH at 90 °C for 1–3 h had specific surface areas as high as 200–300 $m^2\ g^{-1}$ and pores with uniform radii of *ca.* 3 nm. The specific surface area decreased gradually with higher heating temperatures. However, the specific surface areas of the samples from kaolin minerals with low impurities were maintained at 70–110 $m^2\ g^{-1}$ after heating at 1200 °C for 1 h. This high thermal resistance was due to the characteristic microtexture of the γ-Al_2O_3, which consisted of fine γ-Al_2O_3 grains interspaced with residual amorphous silica in the pseudomorph particles of kaolin minerals. Amorphous silica suppressed the γ-$\rightarrow\alpha$-Al_2O_3 phase transition by preventing γ-Al_2O_3 grains from coming into contact and coalescing to give a lower specific surface area.

Air pollution has become more serious in recent years. Pollutants such as NO_x gases, which are mainly generated from automobiles and combustion machines, cause acid rain and photochemical smog. As NO_x gases are generated at high temperatures, thermally resistant catalysts are necessary for their removal.[1] Ceramic materials are expected to find use as catalyst supports to suppress NO_x generation and increase combustion efficiency because of their excellent heat resistance and chemical stability.[2] Of all the porous ceramic materials, γ-Al_2O_3 has been most widely used as a catalyst and catalyst support owing to its large surface area and good thermal stability.[3] γ-Al_2O_3, however, is a metastable phase and its surface area decreases at high temperatures owing to grain growth accompanied with the phase transition to α-Al_2O_3. Therefore, many attempts have been performed to maintain high surface area above 1000 °C. Addition of lanthanum or alkaline-earth metals was effective in maintaining the large surface area at high temperatures because sintering of particles in La-β-Al_2O_3 and $BaO{\cdot}6Al_2O_3$ proceeded more slowly than in γ-Al_2O_3.[4–7] Addition of silica is well known to maintain the large surface area of γ-Al_2O_3 at high temperatures. Highly thermally resistant γ-Al_2O_3 modified with silica has been prepared by various methods.[8–13] Microstructural control of γ-Al_2O_3 is also effective in enhancement of its thermal resistance. Transition alumina with low bulk density, which shows good thermal resistance, has been prepared by fume pyrolysis,[14] hydrothermal treatment[15] and supercritical drying.[16,17]

Recently, we prepared γ-Al_2O_3 with a specific surface area of 200–300 $m^2\ g^{-1}$ and uniform pores of radius *ca.* 3 nm by a novel procedure which we designated as the selective leaching method.[18] In this method, amorphous silica was selectively leached from the pseudomorph particles of calcined kaolin minerals, which consisted of a microtexture of γ-Al_2O_3 particles of fine and uniform size, a so-called spinel phase,[19] in an amorphous silica matrix. Since amorphous silica was interposed between fine γ-Al_2O_3 grains, the γ-Al_2O_3 may be expected to have good thermal resistance. In the other methods stated above, metal alkoxides are often used as starting materials but these are too expensive for industrial mass production. The aim of the present work is to investigate the thermal resistance of γ-Al_2O_3 prepared by the selective leaching method.

Experimental

The starting materials used were synthetic kaolinite (Toyo-Denka-Kogyo, Japan); kaolinites, from Cornwall, UK and from Georgia, USA; dickite from Shokozan, Japan; and halloysite, from Suzuhou, China. The ideal chemical formula of these minerals is $2SiO_2{\cdot}Al_2O_3{\cdot}2H_2O$, except for halloysite, $2SiO_2{\cdot}Al_2O_3{\cdot}4H_2O$.

The samples were calcined at 950 °C for 24 h with heating and cooling rates of 10 and 15 °C min^{-1}, respectively. The calcined samples (3 g) were each dispersed in 250 ml of aqueous KOH at 75 °C for China halloysite and at 90 °C for the other kaolin minerals. Amorphous silica in the samples was selectively leached. The concentration of the KOH solution was 2 M for the synthetic kaolinite and 4 M for the other samples. The leaching time was 3 h for the Shokozan dickite and 1 h for the other samples. After the leaching treatment, the samples were washed with 0.5 M KOH and then washed a further two times with deionized water to remove dissolved ions. Then, the suspension was centrifuged and K^+ ions were further removed using a cation exchange resin [IR-118(H), ORGANO]. The samples were dried at 110 °C for over 15 h in an oven.

The as-prepared samples were heated under the following conditions. In the first series of experiments, the samples were heated at various temperatures between 1100 and 1300 °C at a constant holding time of 1 h. In the second series of experiments, the samples were heated at 1100 °C for various holding times between 1 and 240 h. In these experiments, the samples were placed on a Pt foil. The heating and cooling rates were 15 and 50 °C min^{-1}, respectively.

Powder X-ray diffraction (XRD) patterns were measured using monochromated Cu-Kα radiation with a Rigaku Geigerflex diffractometer. The specific surface area was measured by the BET method using nitrogen gas as adsorbate at −196 °C with a Quanta Chrome Autosorb-1 instrument. The pore size distribution was calculated in the radius range of 1–100 nm by the BJH method[20] using the desorption isotherm. The microtexture of the samples was observed by TEM (H-9000, Hitachi) and the chemical composition was measured using an EDX (H9110 scanning system, Kevex DeltaIII) attached to the TEM. The bulk chemical composition of the samples after the leaching treatment was measured by X-ray fluorescence (RIX3000, Rigaku Denki).

Results and Discussion

Characterization of calcined and leached samples

XRD revealed that the calcined samples comprised γ-Al_2O_3, amorphous silica and other impurity minerals. Weak reflections

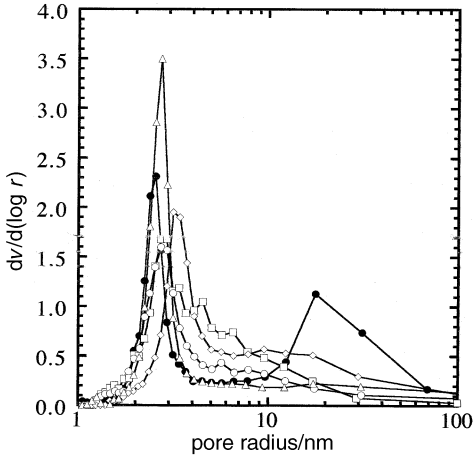

Fig. 1 Pore size distributions of the samples after KOH leaching treatment. (●) Synthetic kaolinite, (◇) Cornwall kaolinite, (△) Georgia kaolinite, (○) Shokozan dickite, (□) China halloysite.

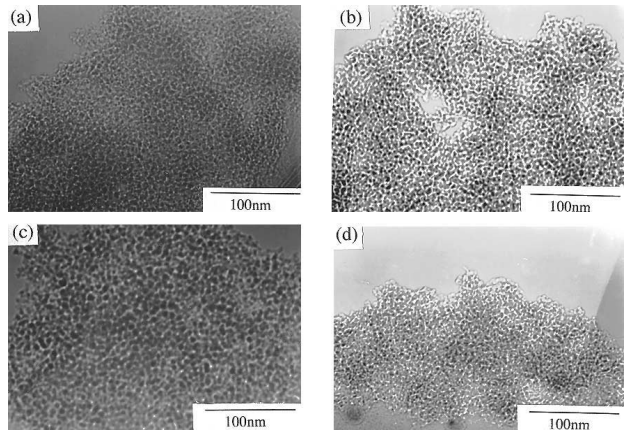

Fig. 2 TEM photographs of the samples after KOH leaching treatment. (a) Synthetic kaolinite, (b) Cornwall kaolinite, (c) Shokozan dickite, (d) China halloysite.

of mullite ($Al_{4+2x}Si_{2-2x}O_{10-x}$) were also identified in the dickite sample. Weak reflections of the following impurity minerals were also identified: quartz (SiO_2) in the synthetic kaolinite; muscovite [$KAl_2(OH)_2Si_3AlO_{10}$] and quartz in the Cornwall kaolinite; anatase (TiO_2) and rutile (TiO_2) in the Georgia kaolinite; and quartz in the halloysite samples.

After the KOH leaching treatment, the height of a halo of amorphous silica in the XRD patterns of the calcined samples decreased and the reflections of mullite in the dickite sample disappeared. On the other hand, the reflections of γ-Al_2O_3 and impurity minerals increased. The specific surface areas of the samples after leaching were 256, 224 and 252 $m^2\ g^{-1}$ for the synthetic, Cornwall and Georgia kaolinites, respectively. The slightly low value of surface area for the Cornwall kaolinite was probably due to the higher amount of impurities, *i.e.* quartz and muscovite. The specific surface areas of the dickite and halloysite samples were 218 and 288 $m^2\ g^{-1}$, respectively. The trend in the surface area of the kaolin group minerals corresponded to the trend in particle size of the starting materials, *i.e.* halloysite < kaolinite < dickite. Fig. 1 shows the pore size distribution curves of these samples. All the samples showed a sharp peak at a radius of *ca.* 2.5–3 nm. These pores were considered to have been formed by the selective leaching of amorphous silica between the γ-Al_2O_3 grains in the pseudomorph particles of the leached samples.[18] As a result, porous γ-Al_2O_3 was obtained by the selective leaching of each kaolin calcined at 950 °C for 24 h. The pore sizes varied little from sample to sample, *i.e.* smallest in the synthetic kaolinite (2.5 nm) and largest in the Cornwall kaolinite sample (3.4 nm). The pores in the Georgia kaolinite sample were of uniform size and showed the sharpest distribution while the pore size of the China halloysite sample showed the widest distribution. Fig. 2(a)–(d) shows TEM photographs of the synthetic kaolinite, Cornwall kaolinite, dickite and halloysite samples. In each sample, the microtexture of the pseudomorph particles consisted of uniform and very fine γ-Al_2O_3 grains. The spaces between the γ-Al_2O_3 grains were observed to be several nm. The 2–3 nm pores in Fig. 1, therefore, were attributed to the spaces formed by the selective leaching of amorphous silica in the pseudomorph particles. The pore size distribution curves of some samples exhibited shoulders at large pore size and that of synthetic kaolinite showed bimodal peaks. The larger pores centred at around 20 nm in radius were considered to be the interparticle pores corresponding to the cavities of agglomerated pseudomorph particles. The pore size distribution curve of the China halloysite sample showed a broad peak at around 4–10 nm besides the peak at *ca.* 2–3 nm. The broad peak was considered to correspond to interparticle pores because the particle size of the China halloysite sample was smaller than that of the other samples.

Thermal resistance of γ-Al_2O_3 prepared by the selective leaching method

Fig. 3 shows changes in the specific surface area of all the samples *vs.* heating temperature (duration of heating = 1 h). When fired at 1100 °C, all the samples maintained specific surface areas of > 150 $m^2\ g^{-1}$. These specific surface areas are apparently higher than that of commercial high-purity γ-Al_2O_3 (Sumitomo, AKP-G015). With higher heating temperatures, the specific surface areas gradually decreased. All the samples except for the Georgia kaolinite sample had specific surface areas as high as 70–110 $m^2\ g^{-1}$ after heating at 1200 °C. Above 1200 °C, there was a decrease in the specific surface areas of all the samples. At 1250 °C, the specific surface area of the Cornwall kaolinite sample was apparently lower than those of the other samples but those of the synthetic kaolinite, dickite and halloysite samples were constant at 40–50 $m^2\ g^{-1}$. At 1300 °C, the specific surface area decreased further and that of the dickite sample showed a maximum value of 30 $m^2\ g^{-1}$. Therefore, there is an apparent difference in the thermal resistance of the five samples. The thermal resistance of these samples is in the order: dickite, synthetic kaolinite ≥ halloysite > Cornwall kaolinite > Georgia kaolinite. It is well known that the $\gamma \rightarrow \alpha$ phase transition of Al_2O_3 causes grain growth and thus reduces the specific surface area. The

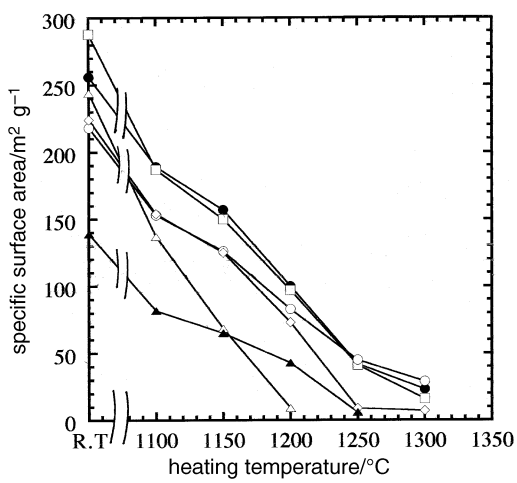

Fig. 3 Plot of specific surface area *vs.* heating temperature for each sample. (●) Synthetic kaolinite, (◇) Cornwall kaolinite, (△) Georgia kaolinite, (○) Shokozan dickite, (□) China halloysite, (▲) high-purity γ-Al_2O_3 (Sumitomo, AKP-G015).

rate of this phase transition is largely dependent on impurities; *e.g.* SiO_2 effectively suppresses the phase transition as mentioned before.[8] By contrast, TiO_2 and Fe_2O_3 impurities accelerate the phase transition.[21] The chemical compositions of the samples after KOH leaching are listed in Table 1. The Georgia and Cornwall kaolinite samples contained a larger amount of TiO_2 and Fe_2O_3 than the other samples. TiO_2 in the Georgia kaolinite sample accelerated the nucleation growth of α-Al_2O_3 especially, which resulted in a drastic decrease of the specific surface area at lower temperatures than in the other samples as shown in Fig. 3. Horiuchi *et al.*[10] reported the thermal resistance of transition aluminas (γ-, δ-, θ-Al_2O_3) at 1100–1400 °C for 5 h. After heating at 1300 °C for 5 h, the specific surface area of high-purity commercial θ-Al_2O_3 with a 2.7–5.2 mass% SiO_2 coating was as high as 23–46 m^2 g^{-1} while that of θ-Al_2O_3 without an SiO_2 coating was <10 m^2 g^{-1}. The thermal resistance of dickite, synthetic kaolinite and China halloysite samples was nearly the same as that of high-purity commercial θ-Al_2O_3 with an SiO_2 coating.

The pore size distribution curves of the samples heated at 1100–1300 °C are shown in Fig. 4(a)–(d). In the synthetic kaolinite sample, the small 2–3 nm pores decreased in number and the pore sizes increased slightly with higher heating temperatures. The peak height corresponding to the small pores decreased at higher temperatures and disappeared above 1200 °C. On the other hand, there was little change in the large 20–30 nm radii pores even after heating at high temperatures. Since the small pores corresponded to inner pores in the pseudomorph particles, the disappearance of the small pores on heating was caused by the collapsing of the microtexture

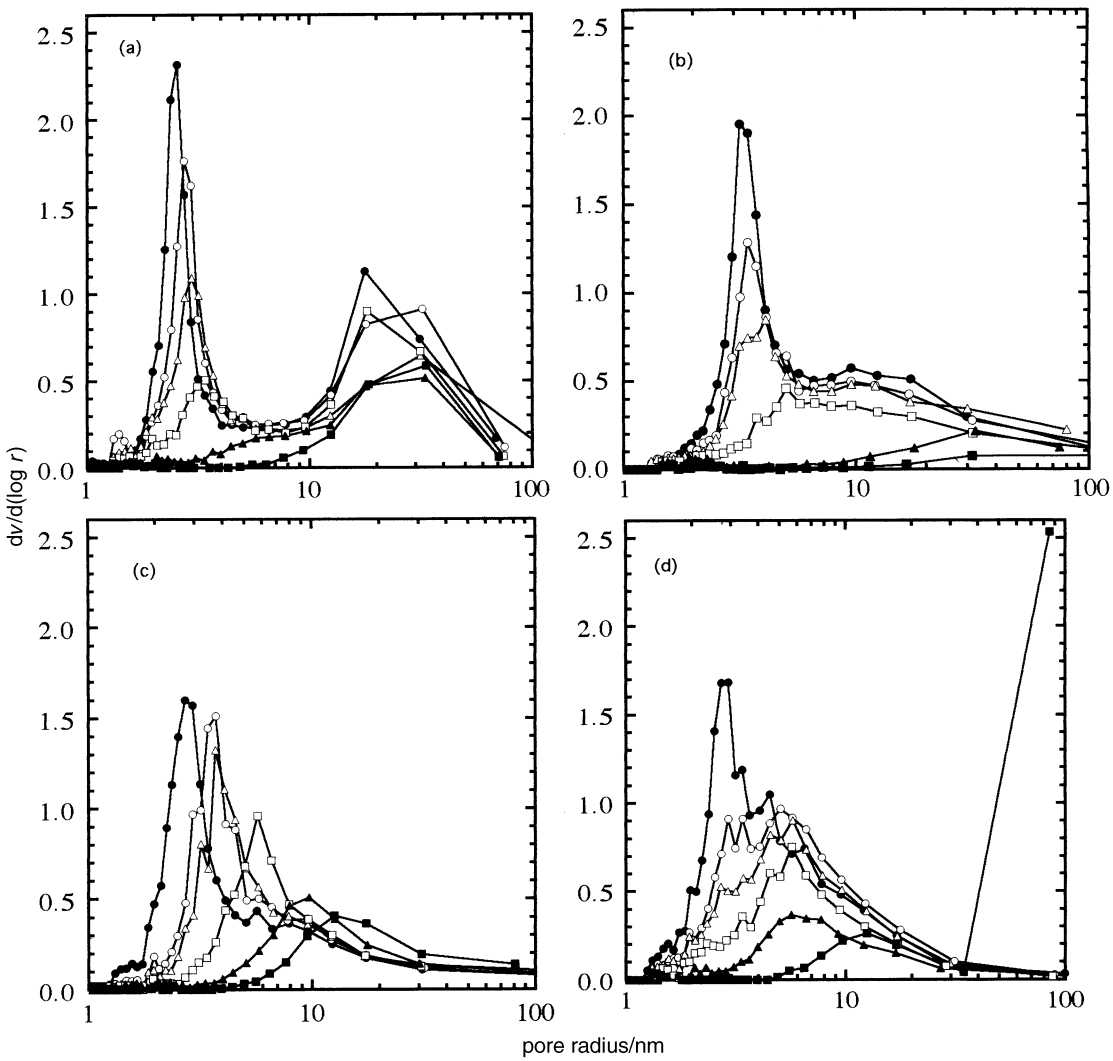

Fig. 4 Pore size distributions of the samples heated at various temperatures. (a) Synthetic kaolinite, (b) Cornwall kaolinite, (c) Shokozan dickite, (d) China halloysite. (●) As prepared, (○) 1100 °C, (△) 1150 °C, (□) 1200 °C, (▲) 1250 °C, (■) 1300 °C.

Table 1 Chemical composition of the samples after KOH leaching

	mass%							
sample	Al_2O_3	SiO_2	K_2O	CaO	MgO	Fe_2O_3	TiO_2	total(%)
synthetic kaolinite	86.0	13.0	0.16	0.05	0.11	0.27	0.37	100.0
Cornwall kaolinite	78.0	16.0	1.4	0.24	0.85	1.2	0.11	97.8
Georgia kaolinite	84.0	6.8	1.4	0.10	0.09	1.0	5.5	98.9
Shokozan dickite	81.0	18.0	0.26	0.06	—	0.18	0.31	99.8
China halloysite	89.0	9.9	0.53	0.06	—	0.29	—	99.8

owing to the rearrangement of γ-Al_2O_3 grains through softening of amorphous silica by a viscous flow mechanism and to grain growth. In the Cornwall kaolinite sample, the small 2–3 nm pores decreased with increasing heating temperatures but a broad peak at 5–20 nm remained, the maximum of which shifted slightly to larger pore sizes. This broad peak, however, disappeared at 1250 °C. In the dickite sample, the small pores of 2–3 nm radius shifted gradually to larger pore sizes with higher temperatures and the pore size distribution curve became broader. At 1200 °C, the maximum shifted to *ca.* 5 nm and the peak height became lower. In the temperature range 1250–1300 °C, the central position of the peak shifted to *ca.* 10 nm and the peak height was even lower. This pore size change can be attributed to grain growth in the pseudomorph particles. In the halloysite sample, the height of the peak at 2–3 nm decreased after heating at 1100 °C and the pores of radius 4–10 nm showed little change. At 1250 °C, the peak at 2–3 nm disappeared and a broad peak remained at *ca.* 4–10 nm. At 1300 °C, this broad peak shifted to larger pore sizes. As a result, there was a small peak at 10–20 nm and a large peak at 100 nm which was the limit of pore size by this pore size distribution analysis method. The 10–20 nm radii pores may have decreased owing to grain growth of alumina grains but large pores may correspond to the pores formed by the sintering of pseudomorph particles.

Fig. 5 shows changes in total pore volume *vs.* heating temperature, *i.e.* 1100–1300 °C for 1 h. In the synthetic kaolinite sample and Shokozan dickite, the total pore volume decreased with higher temperatures. In the Cornwall kaolinite sample, the total pore volume decreased with higher heating temperatures and rapidly so above 1150 °C. In the China halloysite sample, the total pore volume decreased with higher temperatures up to 1250 °C. At 1300 °C, however, the total pore volume was at a maximum because pores with radii >100 nm were formed.

Changes in XRD patterns on heating are shown in Fig. 6(a)–(d). In the synthetic kaolinite sample, transition alumina was largely present in the temperature range 1100–1200 °C. There was also a small amount of mullite and α-Al_2O_3. The amount of mullite and α-Al_2O_3 increased with higher heating temperatures while at 1300 °C, θ-Al_2O_3, α-Al_2O_3, mullite and cristobalite (SiO_2) were identified. Cristobalite is considered to be formed by the crystallization of residual amorphous silica. Quartz impurity reacted with alumina, which resulted in the disappearance of the peaks of quartz. In the Cornwall kaolinite sample, γ-Al_2O_3, quartz and a small amount of mullite were identified. The peaks of muscovite impurity disappeared as it was transformed into an amorphous phase and transition alumina. The amount of mullite increased with higher temperatures. At 1200 °C, peaks of α-Al_2O_3 appeared while at 1250 °C, θ-Al_2O_3 was present while the amount of mullite and α-Al_2O_3 drastically increased. At 1300 °C, the phases present were largely mullite and α-Al_2O_3. In the dickite sample, γ-Al_2O_3 and a small amount of mullite were present before heating while the amount of mullite increased with heating temperature. At 1250 °C, peaks of α-Al_2O_3 appeared while at 1300 °C, θ-Al_2O_3 was present while the amount of α-Al_2O_3 besides mullite increased. In the halloysite sample, transition alumina was identified in the temperature range 1100–1200 °C. At 1250 °C, transition alumina besides mullite and α-Al_2O_3 was also identified. The amount of mullite and α-Al_2O_3 increased drastically at 1300 °C.

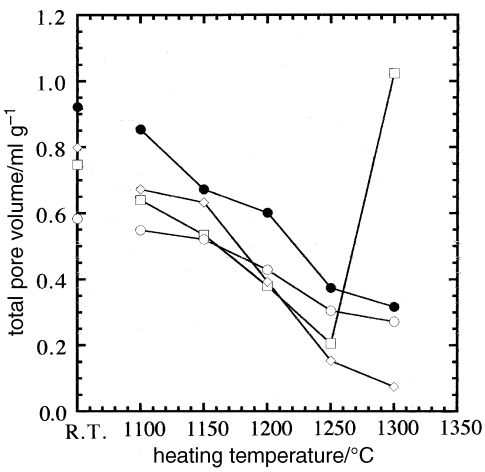

Fig. 5 Change in total pore volumes at 1100–1300 °C for 1 h. (●) Synthetic kaolinite, (◇) Cornwall kaolinite, (△) Georgia kaolinite, (○) Shokozan dickite, (□) China halloysite.

As mentioned above, the changes in the pore size distribution and crystalline phases present were investigated in the temperature range 1100–1300 °C. In the synthetic kaolinite, Cornwall kaolinite and halloysite samples, the peak height at 2–3 nm pore radius decreased with higher heating temperatures while the broad peak at *ca.* 4–20 nm showed little change. Compared to other samples for dickite, the peak at 2–3 nm shifted to larger values. In the synthetic kaolinite and halloysite samples, the predominant phase was largely transition alumina and a little mullite up to 1200 °C. The 2–3 nm pores decreased as the microtexture collapsed because of the growth of γ-Al_2O_3 grains. In the dickite sample, however, the amount of mullite increased with higher temperatures, which caused the 2–3 nm pores to shift to larger sizes.

TEM photographs of samples at 1100–1300 °C are shown in Fig. 7(a)–(d). At 1100 °C, the fine γ-Al_2O_3 grains became slightly larger, resulting in the disappearance of some of the smaller pores. These changes corresponded to the decrease of pores of radii 2–3 nm as shown in Fig. 4. At 1200 °C, for the synthetic kaolinite and halloysite samples, the fine grains became even larger, resulting in the disappearance of more of the smaller pores. In the Cornwall kaolinite sample, the fine grains were larger than those in the synthetic kaolinite and halloysite samples, whereas, in the dickite sample, columnar grains of mullite with sizes ranging from 50 to 200 nm were observed. Therefore, the increase in pores with radii ranging from 5 to 10 nm in the pore size distribution curve was due to the spaces between the mullite grains. For all samples at 1300 °C, the fine grains grew drastically, resulting in the disappearance of the small pores. The results corresponded to the disappearance of the sharp peaks in the pore size distribution curves.

Fig. 8 shows changes in the specific surface areas *vs.* the heating time at 1100 °C. In the synthetic kaolinite, Shokozan dickite and China halloysite samples, the specific surface area decreased gradually with increasing heating time. However, in these samples, the specific surface area became nearly constant at 70–120 m^2 g^{-1} even after heating for 240 h. Fig. 8 also shows changes in the specific surface area of high-purity γ-Al_2O_3 as a reference *vs.* the heating time. All samples except the Georgia kaolinite maintained larger specific surface areas than high-purity γ-Al_2O_3 after heat treatment at 1100 °C for 240 h. Yoldas[8] prepared 1–10 mass% SiO_2-doped γ-Al_2O_3 by the sol–gel method. The 7 and 10 mass% SiO_2-doped γ-Al_2O_3 maintained a specific surface area of *ca.* 100 m^2 g^{-1} after heating at 1100 °C for 100 h. The synthetic kaolinite, Shokozan dickite and China halloysite samples showed higher thermal resistance than SiO_2-doped Al_2O_3 prepared by the sol–gel method. In the Georgia kaolinite sample, the specific surface area decreased very rapidly compared with those of the other samples. In the Cornwall kaolinite sample, the specific surface area decreased more than that in the synthetic kaolinite, dickite and halloysite samples. The Georgia and Cornwall kaolinite samples had a higher content of TiO_2 and Fe_2O_3; the Georgia kaolinite sample in particular having a higher content of TiO_2 than the other samples. Wakao and Hibino[21] reported that

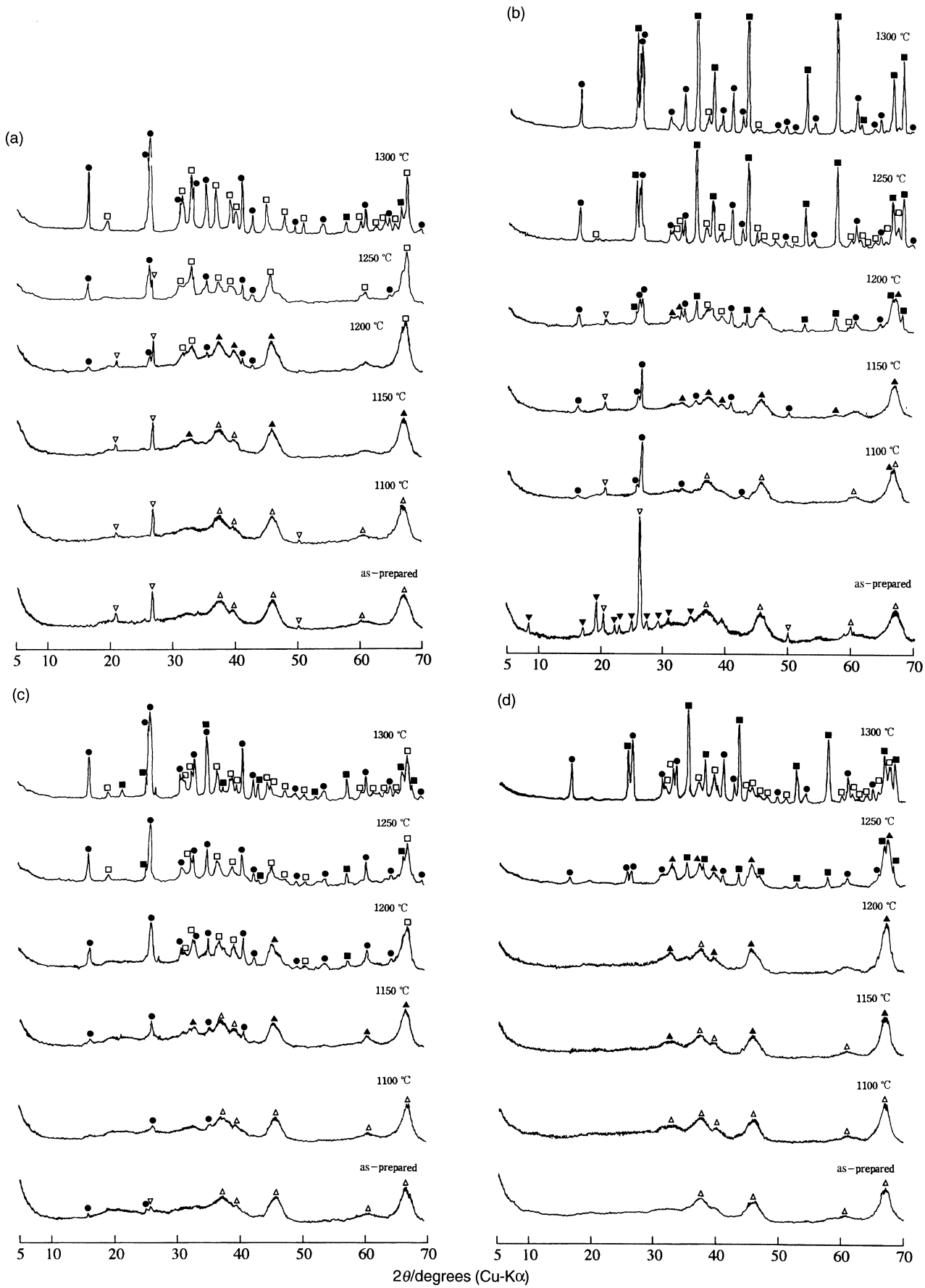

Fig. 6 XRD patterns of the samples heated at 1100–1300 °C for 1 h. (a) Synthetic kaolinite, (b) Cornwall kaolinite, (c) Shokozan dickite, (d) China halloysite. (△) γ-Al_2O_3, (▲) δ-Al_2O_3, (□) θ-Al_2O_3, (■) α-Al_2O_3, (●) mullite, (▽) quartz, (▼) cristobalite.

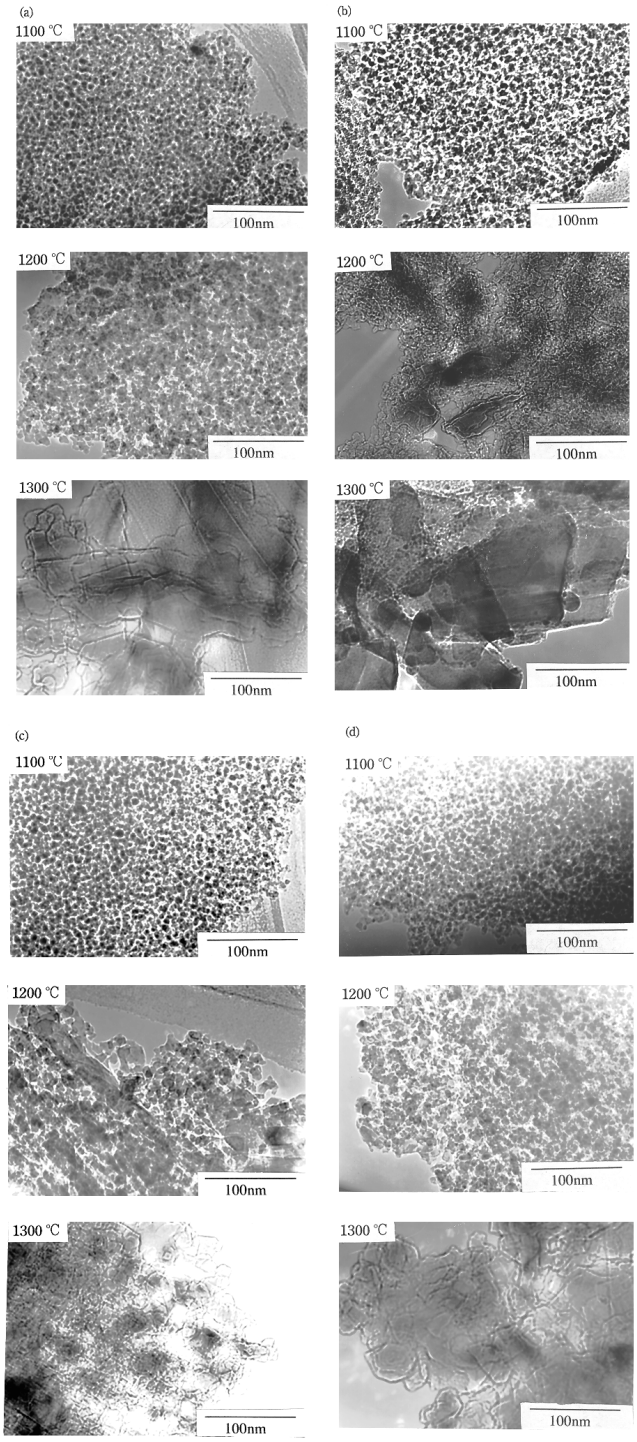

Fig. 7 TEM photographs of the samples after heating at 1100–1300 °C for 1 h. (a) Synthetic kaolinite, (b) Cornwall kaolinite, (c) Shokozan dickite, (d) China halloysite.

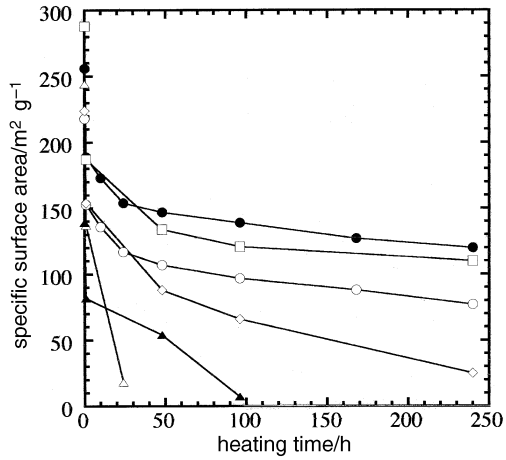

Fig. 8 Plot of specific surface area *vs.* heating time for each sample. (●) Synthetic kaolinite, (◇) Cornwall kaolinite, (△) Georgia kaolinite, (○) Shokozan dickite, (□) China halloysite, (▲) high-purity γ-Al_2O_3 (Sumitomo, AKP-G015).

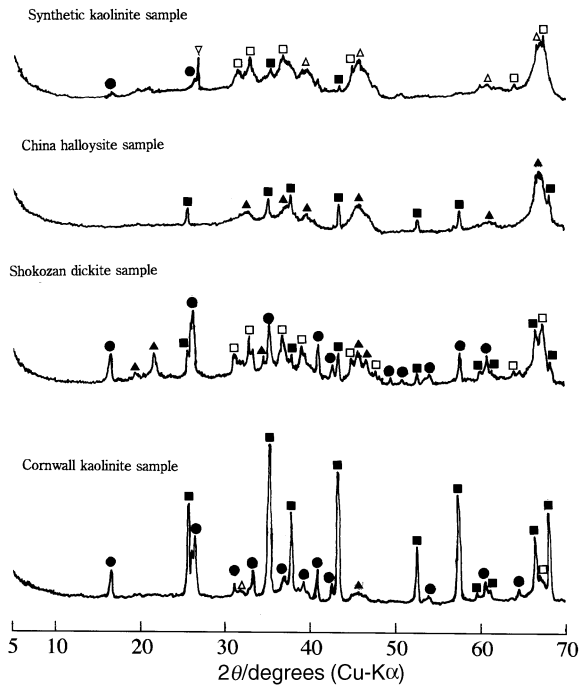

Fig. 9 XRD patterns of the samples heated at 1100 °C for 240 h. (△) γ-Al_2O_3, (▲) δ-Al_2O_3, (□) θ-Al_2O_3, (■) α-Al_2O_3, (●) mullite, (▽) quartz.

TiO_2 and Fe_2O_3 accelerated the γ-→α-Al_2O_3 phase transition. Therefore, in the Georgia kaolinite sample, TiO_2 as impurity, *i.e.*, anatase and rutile, accelerated the γ-→α-Al_2O_3 phase transition, resulting in a drastic decrease of the specific surface area. In the Cornwall kaolinite sample, quartz (crystalline SiO_2) impurity may also influence the rate of phase transition to α-Al_2O_3.

Fig. 9 shows XRD patterns of samples heated at 1100 °C for 240 h. In the synthetic kaolinite and halloysite samples, the predominant phase was largely transition alumina while in the dickite sample, mullite and transition alumina were the main phases. In the Cornwall kaolinite sample, α-Al_2O_3 and mullite were predominant. However, a small amount of transition alumina was present in all the samples and hence enhanced their ability to maintain large surface areas. The fraction of α-Al_2O_3 in the Cornwall kaolinite sample was much larger than in the other samples. As a result, the thermal resistance of γ-Al_2O_3 prepared by the selective leaching of calcined kaolin minerals depended on both the amount and the kind of impurities contained in the starting raw materials. Changes in pore size distributions followed a pattern similar to changes in the heat treatment at 1100–1300 °C for 1 h. Differences in pore size distributions probably depend on the particle size and shape in the starting materials.

As mentioned above, the rate of the γ-→α-Al_2O_3 phase transition in γ-Al_2O_3 obtained from kaolin minerals with a small amount of impurities was much slower than that in commercial high-purity γ-Al_2O_3. The residual amorphous silica was considered to retard the γ-→α-Al_2O_3 phase transition as reported by Yoldas.[8] We consider that the residual amorphous silica prevents γ-Al_2O_3 grains from coming into contact, which results in the retardation of the phase transition to α-Al_2O_3 as

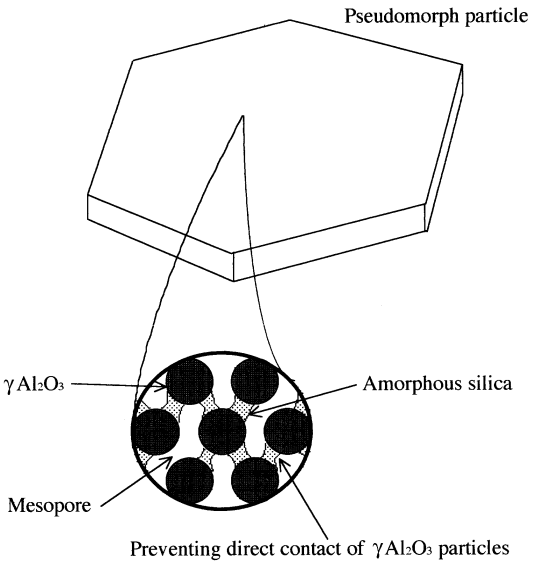

Fig. 10 Schematic illustration of the microtexture of the porous γ-Al_2O_3 prepared by the selective leaching method

shown schematically in Fig. 10. In SiO_2-doped γ-Al_2O_3 prepared by the sol–gel[8] and CVD[13] methods previously reported, the surface of γ-Al_2O_3 particles with an SiO_2-coating is considered to have different surface properties from γ-Al_2O_3. On the other hand, the surface of pores in the present γ-Al_2O_3 samples obtained from calcined kaolin minerals consist of γ-Al_2O_3 grains and amorphous silica. Therefore, it retains the surface properties of γ-Al_2O_3 with high thermal resistance. This is the characteristic feature of the present γ-Al_2O_3 compared with the other highly thermally resistant γ-Al_2O_3 reported previously.

Conclusions

This work has focused on the thermal resistance of mesoporous γ-Al_2O_3 prepared by selective leaching of calcined kaolin minerals. The thermal resistance was examined under two sets of heating conditions. In the first experiment, the γ-Al_2O_3 samples were heated at temperatures from 1100 to 1300 °C for 1 h, while in the second experiment, the heating temperature was fixed at 1100 °C and the heating time was varied from 1 to 240 h. In conclusion: (*i*) heating mesoporous γ-Al_2O_3 obtained from synthesized kaolinite, China halloysite and Shokozan dickite at 1200 °C for 1 h led to a constant specific surface area in the range 70–110 $m^2\ g^{-1}$.

(*ii*) Heating mesoporous γ-Al_2O_3 obtained from synthesized kaolinite, China halloysite and Shokozan dickite at 1100 °C for 240 h led to a specific surface area of 80–120 $m^2\ g^{-1}$.

(*iii*) From the results of the two sets of thermal resistance experiments, the thermal resistances of the mesoporous γ-Al_2O_3 samples were in the following order: Shokozan dickite, synthetic kaolinite ≥ China halloysite > Cornwall kaolinite > Georgia kaolinite, this order being largely related to the amount of impurities such as TiO_2 and Fe_2O_3 in the samples.

(*iv*) By using kaolin minerals containing a small amount of impurities, γ-Al_2O_3 prepared by the selective leaching method had better thermal resistance properties than commercial high-purity γ-Al_2O_3. We consider that residual amorphous silica prevents γ-Al_2O_3 grains from coming into contact, resulting in the retardation of the γ-→α-Al_2O_3 phase transition.

We thank Rigaku Denki Co. Ltd. for measuring X-ray fluorescence. We are also grateful to Dr. Phillip Sawunyama for proof reading this paper. A part of this work was supported by a Grant-in-Aid for Scientific Research (B) (No. 07455263) by the Ministry of Education, Science, Culture and Sports, Japan.

References

1 R. Prasad, L. A. Kennedy and E. Ruckenstein, *Catal. Rev.-Sci. Eng*., 1984, **26**, 1.
2 L. M. Sheppard in *Porous Ceramics: Processing and Applications*, ed. K. Ishizaki, L. Sheppard, S. Okada, T. Hamasaki and B. Huybrechts, (*Ceramic Transactions*, vol. 31, Porous Materials, The American Ceramic Society, Westerville, OH, 1993, p. 3).
3 B. E. Yoldas, *Ceram. Bull*., 1975, **54**, 286.
4 H. Schaper, E. B. M. Doesburg and L. L. Van Reijen, *Appl. Catal*., 1983, **7**, 211.
5 M. Machida, K. Eguchi and H. Arai, *Chem. Lett*., 1986, 151.
6 M. Machida, K. Eguchi and H. Arai, *J. Catal*., 1987, **103**, 385.
7 M. Machida, K. Eguchi and H. Arai, *Bull. Chem. Soc. Jpn*., 1988, **61**, 3659.
8 B. E. Yoldas, *J. Mater. Sci*., 1976, **11**, 465.
9 B. Beguin, E. Garbowski and M. Primet, *J. Catal*., 1991, **127**, 595.
10 T. Horiuchi, T. Sugiyama and T. Mori, *J. Mater. Chem*., 1993, **3**, 861.
11 M. Inoue, H. Otsu, H. Kominami and T. Inui, *J. Mater. Sci. Lett*., 1992, **11**, 269.
12 M. Inoue, H. Kominami and T. Inui, *J. Mater. Sci*., 1994, **29**, 2459.
13 M. Niwa, N. Katada and Y. Murakami, *J. Phys. Chem*., 1990, **94**, 6441.
14 T. Ishikawa, R. Ohashi, H. Nakabayashi, N. Kakuta, A. Ueno and A. Furuta, *J. Catal*., 1992, **134**, 87.
15 T. Fukui and M. Hori, *J. Mater. Sci. Lett*., 1994, **13**, 413.
16 Y. Mizushima and M. Hori, *J. Mater. Res*., 1995, **10**, 1424.
17 Y. Mizushima and M. Hori, *J. Mater. Sci*., 1995, **30**, 1551.
18 K. Okada, H. Kawashima, Y. Saito, S. Hayashi and A. Yasumori, *J. Mater. Chem*., 1995, **5**, 1241.
19 K. Okada, N. Otsuka and J. Ossaka, *J. Am. Ceram. Soc*., 1986, **69**, C251.
20 E. P. Barrett, L. G. Joyner and P. P. Halenda, *J. Am. Chem. Soc*., 1951, **73**, 373.
21 Y. Wakao and T. Hibino, *Nagoya Kogyo Gijutsu Shikensho Hokoku*, 1962, **11**, 588.

Paper 6/05891D; *Received* 27*th August*, 1996